Cosmic rays: current status, historical context

Thomas K. Gaisser
Bartol Research Institute, University of Delaware, Newark, DE 19716, USA

The ISVHECRI conference series emphasizes the connection between high energy physics and cosmic ray physics—the study of elementary particles and nuclei from accelerators in the lab and from space. In this introductory paper on cosmic rays, I comment on several current topics in the field while also providing some historical context.

1. INTRODUCTION

The first meeting in the ISVHECRI (International Symposium on Very High Cosmic Ray Interactions) series was in 1980 in Siberia. It is my belief, however, that the Bartol meeting in 1978 [1] really set the stage for the series by bringing together some key people from particle physics, including Carlo Rubbia, David Cline, J.D. Bjorken, Gaurang Yodh, Larry Jones and Francis Halzen, and from cosmic ray physics, including S. Miyake, C.M.G. Lattes, K. Kamata, Y. Fujimoto, Michael Hillas, K. Niu and W. Vernon Jones. Many of the same people were together at the second conference in the series in 1982 which started in La Paz and ended in Rio de Janeiro [2]. Gaurang Yodh includes a color print of the photo from the Bartol conference in his Hess Lecture presented at Pune in 2005 [3], along with several other historic photos that illustrate his comprehensive review of cosmic rays.

My charge at this conference is to provide introductory comments on the status of cosmic rays. The organization of the paper is conventional, starting with inclusive measurements of atmospheric muons and neutrinos, followed by direct measurements of primary cosmic rays at the top of the atmosphere and finally extensive air shower measurements in the PeV region and above where the intensity is too low for direct observations. Most of these topics are covered in detail in papers presented during the conference. I therefore focus on a few points of interest without attempting a comprehensive review.

2. MUONS AND NEUTRINOS

An approximate analytic expression for the intensity of atmospheric leptons is

$$\begin{aligned}\phi_\iota(E_\iota) \; &= \phi_N(E_\iota)\times \\ &\left\{\frac{A_{\pi\iota}}{1+B_{\pi\iota}\cos\theta\, E_\iota/\epsilon_\pi} + \frac{A_{K\iota}}{1+B_{K\iota}\cos\theta\, E_\iota/\epsilon_K}\right. \\ &\left. + \frac{A_{\mathrm{charm}\,\iota}}{1+B_{\mathrm{charm}\,\iota}\cos\theta\, E_\iota/\epsilon_{\mathrm{charm}}}\right\}, \qquad (1)\end{aligned}$$

where $\phi_N(E_\iota) = dN/d\ln(E_\iota)$ is the primary spectrum of nucleons (N) evaluated at the energy of the lepton (ι). The forms are the same for $\iota = \nu$ and $\iota = \mu$ with different numerical values for the constants $A_{j\iota}$ etc. [4, 5]. The three terms correspond respectively to contributions from decay of pions, kaons and charm [6]. The approximations assume that the primary spectrum of nucleons can be well approximated by a power law, that hadronic cross sections are energy independent, and that inclusive cross sections for hadro-production obey Feynman scaling. The development of this analytical approach dates back 50 years to the early papers of Zatsepin [7] and others. Although detailed simulations are needed in the end, the analytic approximations provide quantitative insight into the physics of atmospheric leptons.

The classic paper of Barrett *et al.* [8] deals with measurements of muons in deep detectors that use the overburden to select muons which had high energy at production in the atmosphere. They describe how the angular dependence of the muon intensity deep underground and its dependence on temperature in the stratosphere depend on the relative contributions of $\pi^\pm$ and $K^\pm$ to the muons. Both effects arise from the competition between decay and re-interaction of the parent hadrons in the upper atmosphere. The expression for the critical energy for meson decay is

$$E_{\mathrm{critical}} \; = \; \frac{\epsilon_j}{\cos\theta^*} \; = \; \frac{m_j c^2 h_0}{\cos\theta^*\, c\tau_j}, \qquad (2)$$

where θ^* is the local zenith angle at lepton production taking account of the curvature of the Earth [5]. The parameters are $\epsilon_\pi \approx 115$ GeV for charged pions as compared to $\epsilon_K \approx 850$ for charged kaons.

2.1. Temperature Dependence

In an isothermal approximation, the density of the atmosphere is described by an exponential with a scale height of $h_0 \approx 6.4$ km, where the numerical value is applicable to the stratosphere where most high-energy muons and neutrinos originate. This numerical value is used to compute the values of ϵ_j in Eq. 2 that appear in the denominator of Eq. 1. From the ideal gas equation relating density and pressure, one finds $h_0 = RT$. Since $\epsilon \propto h_0$, this relation gives rise to a seasonal variation in the rate of muons in a deep

underground detector through the dependence of ϵ in Eq. 1 on h_0. Rates can also reflect sudden changes in the upper atmosphere [9].

The magnitude of the correlation with temperature depends on the muon energy at production and hence on the depth of the detector. Because $\epsilon_K > \epsilon_\pi$, the kaon contribution has a weaker correlation with temperature than the pion contribution, which means that the magnitude of the correlation with temperature depends on the kaon to pion ratio. This dependence has been discussed recently by the MINOS Collaboration in connection with their measurements of cosmic-ray muons [10] in the far detector at Soudan, where the minimum muon energy to reach the detector is approximately 1 TeV. In IceCube the seasonal variation in the muon rate is approximately $\pm 8\%$ [11]. This is an important feature of the background that must be accounted for in interpreting the data.

Rates of atmospheric neutrinos are also expected to vary with temperature [12]. IceCube is large enough so that the rates of TeV neutrinos may be sufficiently high to actually measure their seasonal variation [6]. Since the neutrinos are detected primarily as upward moving ν_μ-induced muons (using the earth as a filter against the downward muon background), the magnitude and phase of their variation will depend on the part of the sky from which they originate.

Because the lifetime of charmed hadrons is so short, their decay products are "prompt." The denominator of the charm contribution in Eq. 1 is unity for $E_\iota < 10$ PeV. As a consequence, the prompt muons and neutrinos are isotropic and have a harder spectrum than decay products of pions and kaons in the energy range above a TeV. These two features have long been used to search for a prompt contribution to atmospheric muons. In Ref. [6] it is pointed out that the lack of seasonal variation is also a signature of the charm channel.

2.2. Muon Charge Ratio

Both MINOS [13] and OPERA [14] are sufficiently deep so that they measure the charge ratio of muons that had energies in the TeV range at production in the atmosphere. The measured increase in the charge ratio from 1.27 below 100 GeV to 1.37 above a TeV reflects the enhanced importance of kaons at high energy. In particular, associated production,

$$p + air \rightarrow \Lambda + K^+ + X, \quad (3)$$

is an important factor in making the $+/-$ charge ratio larger for kaons than for pions. A measurement of the charge ratio by CMS at somewhat lower energy was reported at this conference [15]. The results from MINOS on temperature dependence as well as charge ratio were summarized here by Schreiner [16].

The strong asymmetry of K^+ compared to K^- in the forward fragmentation region (which dominates production of secondaries from a steep spectrum) reflects the fact that the Λ has constituents in common with the incident proton, while there is no corresponding channel for production of K^-. The charmed analog of Eq. 3 is also highly asymmetric [17]. The possible consequence for prompt atmospheric leptons is a subject of current interest.

Analytic expressions for charge separated intensities (μ^+, μ^- and ν_μ, $\bar{\nu}_\mu$) can be constructed in parallel with Eq. 1, as was worked out for pions in Ref. [18]. The charge-sign dependence starts with the separation of neutrons from protons in the primary cosmic-ray beam and tracks the charge dependences of meson production and decay [5].

The new data on temperature dependence and charge sign dependence of atmospheric muons call for a global fit to all the relevant parameters. These include all the spectrum-weighted moments, $Z_{j\iota}$, the attenuation lengths and also the parameters that reflect the initial charge-sign dependence imparted by the fraction of primary nuclei with $Z > 1$ and how this changes with energy.

3. GALACTIC COSMIC RAYS

3.1. Direct measurements of the primary spectrum

Measurements by ATIC [19] and CREAM [20] presented by Seo at this meeting [21] are providing a new and more complex picture of primary composition in the multi-TeV energy region than was generally assumed in the past. In particular, spectra seem to harden somewhat above 200 GeV/nucleon, and there is a hint that the spectrum of helium is somewhat harder than that of protons between 10 and 100 TeV [20].

Figure 1 shows the situation a few years ago. Up to 100 GeV there are rather precise spectrometer measurements of protons and helium from BESS [22], AMS [23], CAPRICE [24] and others. The measurements of BESS and AMS agreed well with each other in normalization as well as spectrum, with proton intensities somewhat higher than CAPRICE and earlier measurements. The line in Fig. 1 is an extrapolation to high energy of the sum of the individual spectra assuming that all are described by a power law with integral spectral index $\gamma = 1.7$. Normalization of protons and helium are to BESS and AMS. Normalization of other nuclei are obtained from HEAO [25] and other measurements as summarized in [26]. The extrapolation comes in on the low side of the indirect measurements with air shower experiments around a PeV, just below the knee.

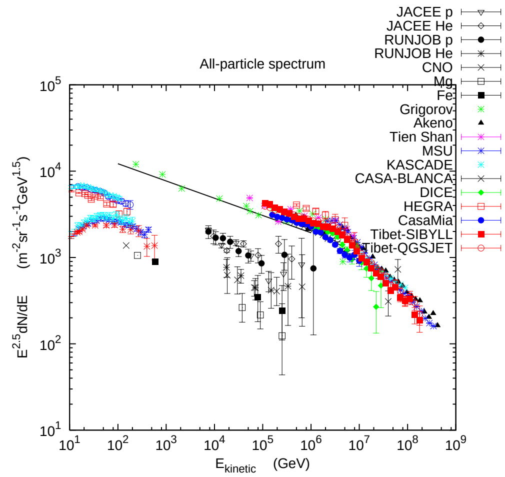

Figure 1: Summary of measurements before 2005.

The plot also shows the early measurements of JACEE and RUNJOB in the region from 10 to several hundred TeV. There was a significant discrepancy between JACEE and RUNJOB for the flux of helium. ATIC-2 and CREAM seem to confirm the higher He intensity of JACEE. Adding together the CREAM measurements of protons, helium and heavier nuclei gives a higher all-particle intensity around 100 TeV in better agreement with the TIBET air shower measurement. The harder spectrum reported by CREAM in the range 10 - 100 TeV/nucleus when extrapolated to the knee region leads to this improved agreement.

3.2. Knee of the spectrum

Fifty years ago Peters [27] suggested that the steepening in the knee region may be associated with the upper end of the spectrum of particles from the dominant source of cosmic rays, which could be powered by supernovas. He explained the relatively smooth behavior of the cutoff as a consequence of different primary nuclei having cutoffs at different energy per particle under the assumption that the underlying effect depends on magnetic rigidity. The definition of rigidity, $R(Z) = Pc/Ze$, provides the scaling relation between total energy ($E \approx Pc$) and the charge Ze of nuclei moving in a given configuration of magnetic fields. If the "cutoff" of the spectrum occurs at a characteristic rigidity, R_c, then protons bend first at $E_c = eR_c$ followed by helium at $2eR_c$, carbon at $6eR_c$ up to iron at $26eR_c$. This sequence is sometimes referred to as a "Peters cycle". The KASCADE Experiment [28] provided the first observation of this sequence of changes in the knee region, with protons steepening first then helium and then heavier nuclei. The relative abundances of various nuclei inferred from the KASCADE data depends on the interaction model used for simulation necessary to unfold the spectra. However, helium appears more abundant than protons above 1 PeV whether SIBYLL or QGSjet is used for the unfolding. This feature is qualitatively consistent with an extrapolation of the direct measurements assuming a harder spectrum for helium than for protons.

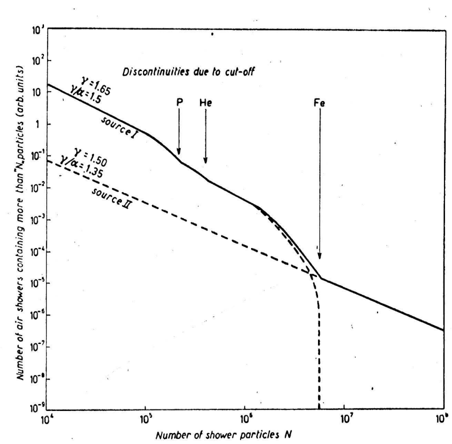

Figure 2: Two component concept of Peters (1960).

Already at the time of Peters' paper the spectrum was known to continue beyond the knee. He suggested a second population with a significantly smaller total number of particles but with a slightly harder spectrum that continues to higher energy, as shown in Fig. 2 from his paper. We now know, however, that the spectrum continues for three orders of magnitude after the knee with a *steeper* spectrum than below the knee. Not until the ankle does the spectrum harden in the way expected by Peters. At least one additional Peters cycle with a cutoff at higher energy is needed to fill in the gap between the knee and the ankle. Hillas [29] calls this "Component B".

3.3. Component B

The question of the cosmic-ray spectrum above the knee was extensively discussed at the two meetings on "Physics at the end of the Galactic cosmic ray spectrum" in Aspen in 2005 and 2007. Figure 3 illustrates the discussion with schematic outlines of three separate components superimposed on the plot of the spectrum from the review of Nagano and Watson [30]. In this scheme, the second knee is a cutoff associated with a second population of Galactic sources of unknown origin, and the extra-galactic component dominates only above the ankle. It is interesting that the new spectrum of KASCADE-Grande presented at this conference [31] shows a concavity just above 10 PeV that could be interpreted as the onset of Component B.

Another point is to estimate the power required to produce the B-component. The desired result is obtained by integrating the spectrum of the B compo-

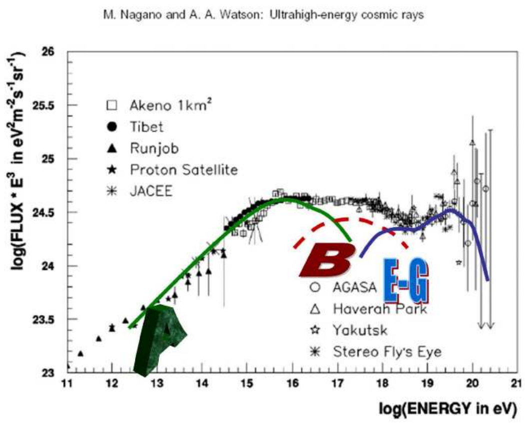

Figure 3: Schematic picture showing three populations of cosmic rays: $\mathcal{A}$ is the dominant galactic component, perhaps accelerated directly by supernova remnants; $\mathcal{B}$ is a higher-energy galactic population of uncertain origin; $\mathcal{E}-\mathcal{G}$ is the extra-galactic component that dominates above the ankle around 3 EeV.

nent weighted by an estimate of the lifetime of high-energy cosmic rays in the galaxy. The expression

$$\mathcal{L} \;=\; V_G\,\frac{4\pi}{c}\int E\,\frac{1}{\tau(E)}\,\frac{\mathrm{d}N}{\mathrm{d}E}\mathrm{d}E \tag{4}$$

gives the total power in the sources to supply this component. Taking

$$\tau_{esc} = 2\times 10^{7}\,\mathrm{yrs}\,E^{-0.33}, \tag{5}$$
$$V_{Galaxy} \;=\; 3\times 10^{66}\,\mathrm{cm}^3 \tag{6}$$

and a differential source spectral index below the cut-off of $\gamma+1=-2.1$, leads to a power requirement of $\sim 2\times 10^{39}$ erg/s.

3.4. Acceleration mechanisms

Another topic featured at the Aspen meetings was a discussion of acceleration mechanisms. The classic estimate of the upper limiting energy of acceleration by shocks driven into the interstellar medium by expanding supernova remnants is $E_{\max}\approx 100\,\mathrm{TeV}$ for protons [32]. Two aspects of non-linear shock acceleration are important for building a synoptic picture of Galactic cosmic rays. One is the amplification of magnetic fields near the shock [33], which increases $E_{\max}\propto ZeBR$. This allows diffusive acceleration driven by supernova remnants to accelerate particles to a maximum rigidity one PV or higher, as would be expected if the knee is related to the upper limit of the dominant population of Galactic cosmic rays.

The other important effect is the concavity introduced by the cosmic-ray pressure of the highest energy particles on the plasma upstream of the shock. The result is that higher energy particles experience a larger velocity difference than the canonical factor of 4 at the sub-shock. In diffusive shock acceleration, the integral spectral index γ is related to the ratio of velocity of the upstream flow into the acceleration region (u_1) to the downstream velocity (u_2) by

$$\gamma \;=\; \frac{3}{u_1/u_2\,-1}. \tag{7}$$

In the non-linear case, $u_1(d)$ is a function of distance upstream of the shock, with $u_1(d)/u_2$ increasing as d increases. Higher energy particles can diffuse further upstream on average before reversing direction; hence the concave nature of the spectrum [34].

Non-linear diffusive shock acceleration is contrasted with the test-particle approximation in which the effect of the accelerated particles on the plasma flowing through the shock is neglected. Then, for a strong shock, $u_1/u_2=4$ and $\gamma=1$, which produces a spectrum with equal energy content per logarithmic interval on energy. In the non-linear case, most of the energy of the accelerated spectrum is near $E_{\max}$. An interesting idea that uses this feature is the proposal by Ptuskin & Zirakashvili [35]. At each epoch in the evolution of a supernova remnant, most of the power goes into particles at the highest possible energy. As the remnant evolves, $E_{\max}$ decreases and the highest energy particles can then escape upstream (that is, to the outside). The spectrum produced by a supernova over its lifetime is then the sum of the contribution from each epoch.

A full picture of the sources, acceleration and propagation of galactic cosmic rays does not yet exist. What seems likely to me, however, is that in reality there are many sources with different spectra and capable of accelerating particles to different maximum energies. The complex structure of the spectrum indicated by the CREAM results below 100 TeV and by the KASCADE-Grande results in the air shower range may reflect such underlying complexity.

4. EXTRAGALACTIC COSMIC RAYS

A well-known alternative to the picture described in the previous section and summarized in Fig. 3 is that of Berezinsky and collaborators [36]. They explain the ankle as a consequence of energy loss by protons due to $e^{\pm}$ pair production on the cosmic background radiation. Such a model requires that the extra-galactic component consists primarily of protons and that there is a cosmological distribution of sources capable of accelerating particles to energies above 100 EeV. In this picture the extra-galactic population dominates down to ~ 300 PeV and a galactic B component is not needed. A signature would be a transition in the composition from heavy nuclei at the end of the galactic population to protons that dominate the extra-galactic component in this model.

4.1. Composition

Results from HiRes [37] and HiRes-MIA [38] do indicate a transition from heavy nuclei below 300 PeV to protons in the EeV range and above. But the question is unsettled because Auger results [39] indicate on the contrary that the composition above 10 EeV is mostly heavy nuclei.

The two contrasting pictures of the transition from galactic to extra-galactic cosmic rays and their relation to composition have been discussed in a series of papers by Allard *et al.* [40]. In the case of a mixed composition at the source, even if there is a preponderance of heavy nuclei, a significant fraction of protons is expected at Earth as a result of photo-nuclear disintegration during propagation through the microwave background, provided that the sources have a cosmological distribution and accelerate particles to sufficiently high energy. In any case, this picture would also be difficult to reconcile with the Auger results on composition because there would be large fluctuations in the Xmax distribution as a consequence of the mixed composition after propagation to Earth (protons and iron).

There is considerable experimental activity to explore the transition region. Low-energy extensions of Auger are now in operation [41], and the low-energy extension of the telescope array is under construction [42]. Meanwhile, KASCADE-Grande [31], IceCube [43] and TUNKA [44] are reaching the transition region from below. Concerning the discrepancy in composition between HiRes and Auger, it may be relevant to note that the selection of events is somewhat different in the two cases. HiRes reconstructs event trajectories using two Fly's Eyes in stereo, while the Auger reconstruction uses a hybrid technique that involves times of hits in one or more surface detectors along with the fluorescence signal. Some insight on the differences may come from the Telescope Array [45], which is also a hybrid detector.

4.2. Two generic models

One possibility is a machine in which the magnetic fields required for acceleration are strong enough and in an appropriate configuration so that accelerated protons and nuclei lose energy in the ambient radiation fields by photo production and photo disintegration respectively before they escape from the system. The acceleration time scale has to be short or comparable to the photo-interaction rate. Then if the escape time for neutrons is short compared to their photo-interaction time scale they will escape and contribute to the population of cosmic rays. In this class of models the extra-galactic cosmic rays would be protons from decay of the escaping neutrons.

In addition, neutrinos produced in the same sources

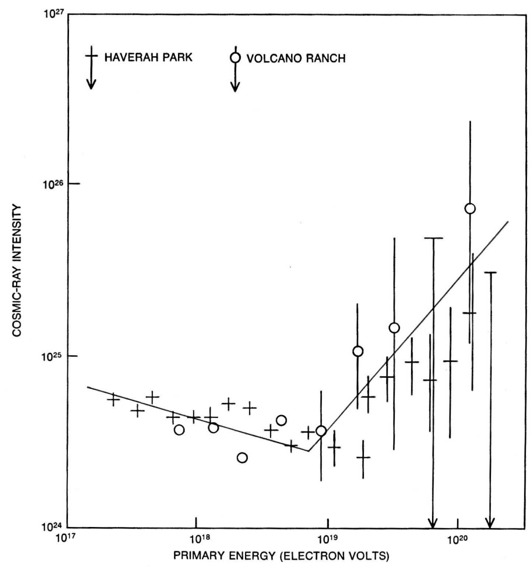

Figure 4: Summary of primary spectrum measurements from Linsley's review [51].

in reaction chains like

$$p + \gamma \to n + \pi^+ \to n + \mu^+ + \nu_\mu \qquad (8)$$

will then have a spectrum and intensity related by kinematics to that of the cosmic-rays. This class of models would be a realization of the Waxman-Bahcall limit [46]. Ahlers *et al.* [47] point out that the limits from IceCube already constrain models of this type.

A contrasting possibility is that the extra-galactic cosmic rays could be powered by shocks driven into an external environment. In this case, whatever material is available would be accelerated, in analogy with galactic cosmic rays accelerated in shocks driven by supernova explosions. External shocks driven by gamma-ray bursts or jets of active galaxies [48] could be realizations of this class of models. The composition could be mixed and there would be no particular reason to expect a high intensity of neutrinos or gamma-rays from interactions of the accelerated particles.

4.3. The end of the cosmic-ray spectrum

The experimental discovery of extra-galactic cosmic rays can be attributed to the Volcano Ranch experiment, built by John Linsley and Livio Scarsi starting in 1958 [49]. The array was spread over an area of approximately 8 km^2. In 1962 they detected an event estimated to have an energy of 10^{20} eV (with large uncertainty), too high to be contained in the galaxy [50]. In his 1978 review of ultra-high energy cosmic rays, Linsley [51] combined data from Volcano Ranch and Haverah Park [52] in the U.K. into a plot that shows

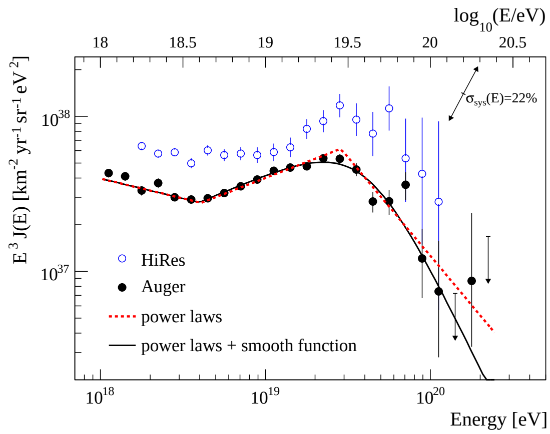

Figure 5: HiRes and Auger spectrum measurements from Ref. [57].

the ankle of the spectrum, which he interpreted as the onset of extragalactic cosmic rays. Linsley's figure is reproduced here as Figure 4. The data clearly show the ankle but no sign of the suppression expected from photo-production interactions in the microwave background if the highest energy particles come from a cosmological distribution of sources.

Linsley's review came at an important time in the history of measurements of ultra-high-energy cosmic rays. The Fly's Eye detector was under construction at Dugway Proving Ground in Utah after the technique had been demonstrated for the first time by using three new Fly's Eye receivers at the Volcano Ranch array to see the fluorescence light from air showers in coincidence with Linsley's ground array. [53].

It was another thirty years until HiRes, using the Fly's Eye technique, showed a drop in the spectrum [54] consistent with that predicted by Greisen [55] and Zatsepin & Kuz'min [56]. The HiRes result is shown in Fig. 5 along with the latest spectrum from the Auger detector [57]. The two spectra agree well with each other within the uncertainties of the energy calibration, which are of the order of 20%. Moving one of the sets of points along the direction of the slanted arrow brings the two measurements into agreement. In fact this point illustrates the possibility noted already by Linsley of using the GZK feature to calibrate the energy assignment.

4.4. Anisotropy?

Linsley also pointed out that protons with energies of the order of 100 EeV would have sufficiently high rigidity to be likely to point back to their sources within ~ 100 Mpc. In this connection it is interesting to compare the sky plot in Linsley's review with that of the Auger experiment. Linsley shows the directions of 16 events with energy greater than 50 EeV measured by Haverah Park [58]. He points out that a significant fraction of the events come in from directions at large angle to the galactic plane, which argues in favor of an extragalactic origin if the particles are protons with high rigidity. The first Auger sky plot published in 2007 [59] showed a rather strong correlation of events with $E \geq 57$ EeV with the large scale distribution of matter in the nearby universe as traced by AGNs. Since then the significance of the correlation has decreased [60], but it is still suggestive of a correlation of the kind that might be expected if the sources are correlated with the large-scale distribution of matter [61] and if the particles in this energy range are mostly protons.

In this connection, it is important to note that the measurement showing heavy composition extends only up to 40 EeV and does not yet overlap with the event sample used to look for anisotropy. In a recent paper, Calvez, Kusenko and Nagataki [62] suggest that GRBs in the Milky Way on a 10^5 year time scale could contribute to the pool of cosmic rays above 10 EeV. This would be a kind of second "B component" that would explain the heavy composition of Auger as the end of the highest energy galactic Peters cycle. The onset of the true extragalactic component would then be around 50 EeV. The challenge is to find ways to increase the statistics and precision of measurements of cosmic rays up to 100 EeV despite the extremely low intensity of such particles.

4.5. End of the spectrum revisited

Finally, it is salutary to remember the Hillas plot [63]. In his iconic diagram, Hillas places potential sources in a space defined by their sizes and magnetic fields. A remarkable feature of the plot is that the few sources capable of accelerating particles to 100 EeV are not far above the line. A realistic possibility is, therefore, that the steepening of the spectrum may to some extent reflect a cutoff at the accelerators as well as (or instead of) the effect of energy losses to interactions with photons of the cosmic microwave background.

Acknowledgments

I am grateful to Adrienne Kolb and Eun-Joo Ahn for an enlightening visit to the Fermilab archive. I thank Larry Jones for information about the ISVHECRI conference series and Ralph Engel for bringing Reference [62] to my attention. I thank Todor Stanev for reading this paper in draft form and Hank Glass for generous editorial assistance with this paper. Much of the material for this paper was developed during my stay in Germany with financial support from the Humboldt Foundation. My work is also supported in part by the U.S. Department of Energy under contract DE-FG02-91ER40626.

References

[1] *Cosmic Rays and Particle Physics–1978*, (A.I.P. Conf. Proc. #49), ed. T.K. Gaisser, 1978.
[2] *Workshops on Cosmic Ray Interactions and High Energy Results*, ed. C.M.G. Lattes, 1982.
[3] Gaurang Yodh, Hess Lecture, 29th International Cosmic Ray Conference Pune (2005) 10, 13-36.
[4] *Cosmic Rays and Particle Physics*, Thomas K. Gaisser (Cambridge University Press, 1990).
[5] Paolo Lipari, Astropart. Phys. 1 (1993) 195.
[6] Paolo Desiati & Thomas K. Gaisser, Phys. Rev. Lett. 105 (2010) 121102.
[7] G.T. Zatsepin & V.A. Kuz'min, Soviet Physics JETP 12 (1961) 1171.
[8] P. Barrett, et al., Revs. Mod. Phys. 24 (1952) 133.
[9] S. Osprey et al., Geophysical Research Letters 36 (2009) LD5809.
[10] P. Adamson et al., Phys. Rev. D 81 (2010) 012001.
[11] Serap Tilav et al., Proc. 31st Int. Cosmic Ray Conf. (Lodz, 2009), arXiv:1001.0776.
[12] Elisa Bernardini & Markus Ackermann, Proc. 29th Int. Cosmic Ray Conf. (Pune, India, 2005).
[13] P. Adamson et al., Phys. Rev. D 76 (2007) 052003.
[14] OPERA Collaboration, arXiv:1003.1907.
[15] Gavin Hesketh, this conference.
[16] Philip Schreiner, this conference.
[17] F.G. Garcia et al., Phys. Lett. B528 (2002) 49.
[18] W.R. Frazer et al., Phys. Rev. D5 (1972) 1653.
[19] A.D. Panov et al., Bulletin of the Russian Academy of Sciences:Physics, 71 (2007) 494.
[20] H.S. Ahn et al., Astrophys. J. Letters 714 (2010) L89.
[21] Eun-Suk Seo, this conference.
[22] T. Sanuki et al., Astrophys. J. 545 (2000) 1135.
[23] AMS Collaboration, Phys. Letters B 490 (2000) 27; B 494 (2000) 193.
[24] M. Boezio et al., Astropart. Phys. 19 (2003) 583.
[25] J.J. Engelmann et al., Astron. & Astrophys. 233 (1990) 96.
[26] K. Nakamura et al. (Particle Data Group), J. Phys. G 37 (2010) 075021 (Review #24, *Cosmic Rays*).
[27] B. Peters, Il Nuovo Cimento XXII (1961) 800-819. Also, Proc of the Moscow Cosmic Ray Conference, quoted by Peters as Vol. VIII, 157 (July 1960).
[28] T. Antoni et al., Astropart. Phys. 24 (2005) 1.
[29] A.M. Hillas, arXiv:astro-ph/0607109.
[30] M. Nagano & A.A. Watson, Revs. Mod. Phys. 72 (2000) 689.
[31] J.C. Arteaga-Velázquez *et al.*, this conference and arXiv:1009.4716.
[32] P.O. Lagage & C.J. Cesarsky, Astron. Astrophys. 118 (1983) 223 and 125 (1983) 249.
[33] A.R. Bell, Monthly Not. Royal Astron. Soc. 353 (2004) 550.
[34] E. Amato, P. Blasi & S. Gabici, Monthly Not. Royal Astron. Soc. 385 (2008) 1946. See also D. Caprioli, E. Amato & P. Blasi, Astropart. Phys. 33 (2010) 307.
[35] V.S. Ptuskin & V.N. Zirakashvili, Astron. & Astrophys. 429 (2005) 755.
[36] V. Berezinsky, A.Z. Gazizov & S.I. Grigorieva, Phys. Rev. D 74 (2006) 043005.
[37] R.U. Abbasi et al., Phys. Rev. Letters 104 (2010) 161101.
[38] R.U. Abbasi et al., Astrophys. J. 622 (2005) 910.
[39] J. Abraham et al., Phys. Rev. Letters 104 (2010) 091101.
[40] D. Allard, A. Parizot & A.V. Olinto, Astropart. Phys. 27 (2007) 61.
[41] A. Etchegoyen, arXiv:1004.2635.
[42] http://www.telescopearray.org/papers/wp015.pdf
[43] Fabian Kislat, Proc. European Cosmic Ray Symposium, 2010; Tilo Waldenmaier, Proc. ICATPP Conference on Cosmic Rays for Particle and Astroparticle Physics; S. Tilav, this conference.
[44] N.M. Budnev et al., Proc. 31st Int. Cosmic Ray Conf. (Ldz, Poland, July 2009, paper #1069).
[45] J.N. Matthews, Proc. 31st Int. Cosmic Ray Conf. (Ldz, Poland, July 2009, paper #1386); M. Fukushima, this conference.
[46] Eli Waxman & John Bahcall, Phys. Rev. D 59 (1998) 023002.
[47] Markus Ahlers, Luis A. Anchordoqui & Subir Sarkar, Phys. Rev. D 79 (2009) 083009.
[48] E.G. Berezhko, Astrophys. J. Letters, 684 (2008) L69.
[49] John Linsley's papers are in the Fermilab archives. The first Volcano Ranch notebook dated June, 1958 describes difficulties shipping equipment by truck from M.I.T., the arrival of Livio Scarsi and an encounter with a rattle snake, as well as the installation of power for the detector.
[50] John Linsley, Phys. Rev. Letters 10 (1963) 146.
[51] John Linsley, Scientific American 239, July, 1978.
[52] M.A. Lawrence, R.J.O. Reid & A.A. Watson, J. Phys. G 17 (1991) 733.
[53] H.E. Bergeson et al., Phys. Rev. Letters 39 (1977) 847.
[54] R.U. Abbasi et al., Phys. Rev. Letters 100 (2008) 101101.
[55] K. Greisen, Phys. Rev. Letters 16 (1966) 748.
[56] G.T. Zatsepin & V.A. Kuz'min, Sov. Phys. JETP Letters 4 (1966) 78.
[57] Pierre Auger Collaboration, Phys. Lett. B685: (2010) 239-246.
[58] For a summary of investigations of directions of UHECR before 2000, see the review of Nagano and Watson [30].
[59] Pierre Auger Collaboration, Science 318 (2007) 938.

[60] P. Abreu et al., arXiv:1009.1855v2 (to appear in Astroparticle Physics).
[61] Todor Stanev et al., Phys. Rev. Letters 75 (1995) 3056.
[62] A. Calvez, A. Kusenko & S. Nagataki, arXiv:1004.2535v2.
[63] A.M. Hillas, Ann. Rev. Astron. Astrophys. 22 (1984) 425.